Available online at www.sciencedirect.com
SCIENCE DIRECT®
Applied Clay Science 22 (2003) 279–293
Applied CLAY Science
www.elsevier.com/locate/clay

Swelling–shrinkage kinetics of MX80 bentonite

G. Montes-H[a,*], J. Duplay[a], L. Martinez[b], C. Mendoza[c]

[a] UMR 7517 ULP–CNRS, CGS, 1 rue Blessig, F-67084 Strasbourg, France
[b] UMR G2R/7566, UHP Nancy 1, BP 239, 54506 Vandoeuvre CEDEX, France
[c] LDFC UMR 7506, Institute de Physique, 3 rue de l'Université, 67084 Strasbourg, France

Received 16 July 2002; received in revised form 21 February 2003; accepted 6 March 2003

Abstract

The swelling–shrinkage kinetic of an industrial Bentonite (MX80) was investigated using a new technique of environmental scanning electron microscopy (ESEM) coupled with a digital image analysis (DIA) program (Visilog). This expansive clay was characterized by several analytic tools (ICP-AES, SEM, STEM, XRD, etc.), before applying the new ESEM technique.

The swelling–shrinkage was directly observed at high magnification and at different relative humidity states in an ESEM. Nine wetting/drying cycles were performed on the sample. Each cycle was performed at different relative humidities (55%, 60%, 65%, 70%, 75%, 80%, 85%, 90%, and 95%).

A DIA program was used to determine swelling–shrinkage. This method consists of estimating the percent augmentation of the surface as a function of time.

Finally, a swelling–shrinkage kinetic model was tested, based on a first-order linear kinetic equation.

The results show that the coupled ESEM and DIA can be a powerful method of estimating the swelling/shrinkage potential of expansive clays. The exponential model fits well with the experimental data.

Keywords: Swelling; Shrinkage; Kinetic; Bentonite; ESEM; Analysis digital image

1. Introduction

The industrial and environmental uses of clays are expanding every year. For example, it is estimated that about 8 million tons of the bentonites were used in 1992 throughout the world (Murray, 2000). One of the principal applications for bentonite is in drilling muds. However, it is widely used as a suspending and stabilizing agent, and as an adsorbent or clarifying agent, in many industries. Recently, bentonite was proposed as a barrier protection in nuclear waste storage thanks to its very high swelling–shrinkage and water adsorption potentials (Pusch, 1992; Al-Tabbaa and Aravinthan, 1998). This makes, the estimation of the swelling–shrinkage potential of expansive clays in the laboratory very important. The methods available for the estimation of the swelling–shrinkage potential are grouped into two categories: physico-chemical and mechanical methods. The common analytical techniques used in physico-chemical methods are the X-ray diffusion

* Corresponding author. Fax: +33-388367235.
E-mail addresses: montes@illite.u-strasbg.fr, german_montes@hotmail.com (G. Montes-H).

0169-1317/03/$ - see front matter © 2003 Elsevier Science B.V. All rights reserved.
doi:10.1016/S0169-1317(03)00120-0

at small angles, X-ray diffraction, scanning transmission electron microscopy (STEM) and imbibition. On the other hand, the classic experimental techniques used in the mechanical methods are the consolidometer test and the soil suction test (Parcevaux, 1980; Abdullah et al., 1999; Al-Rawas, 1998; Komine and Ogata, 1994).

This study proposes a new technique to estimate the swelling–shrinkage potential using a kinetic procedure by environmental scanning electron microscopy (ESEM) coupled with the digital images analysis (DIA) program.

The ESEM was introduced in the last decade. It differs from conventional Scanning Electron Microscope on the permitted presence of a low vacuum in the sample chamber. Thus, wet, oily, dirty, or non-conductive samples can be examined in their natural state without modification or preparation (Jenkins and Donald, 2000). The sample environment can be varied through a range of pressures or temperatures (Baker et al., 1995).

The sample temperature ranging from −5 to 55 °C is controlled by a "cooling stage" installed on the ESEM. A differential pumping system permits also the control of the ESEM chamber pressure ranging from 0.1 to 10 Torr. These combined factors make the ESEM a powerful tool for investigating the in situ interactions between clay minerals and water.

The ESEM was used specifically to directly observe, at high magnification, the effect of the freshwater hydration on bentonite morphology "in general bentonite aggregates". Free swell tests show that the "bentonite aggregates" swell intensively on contact with fresh water (Montes-H, 2002). We have performed in this study experiments to observe the swelling–shrinkage of an industrial bentonite (isolated aggregates). The swelling–shrinkage quantification is achieved using a digital image analysis program (Visilog 5.3). This digital image analysis consists of an estimate of the swelling–shrinkage surface as a function of time.

Finally, two exponential models were applied to fit the experimental data. For this it was necessary to consider that the swelling–shrinkage is equi-dimensional. This supposition seems logical considering the scale of aggregates in expansive clays (Montes-H, 2002).

2. Experimental methods

2.1. Bentonite characterization

The classical methods were used to estimate the mineralogy of the MX80 bentonite. In fact, the complete characterization was achieved by different French laboratories (LEM-CREGU). The description of each analytical technique is not considered in this study.

XRD analysis was carried out directly on bentonite-raw (minerals identification) and oriented clay fraction "<2 μm" (identification of clay family). A comparative analysis with the X-ray diffractogram corresponding to clay mineral permitted to identify the quartz and the montmorillonite as the main mineral phases. In addition the X-ray diffractogram corresponding to the clay fraction shows that the clay family corresponds to a typical smectite "montmorillonite", since the ethylene glycol test shows a shift of the 12 Å peak up to 17.14 Å. The 12 Å peak is closed up to 9.66 Å when the sample is dried at 490 °C.

The clay fraction morphology and chemical composition were studied by means of STEM and ICP-AES. STEM analysis shows folded particles and turbostratic sheets stacking. The average chem-

Table 1
Mineral composition of the MX80 bentonite

	Proportion (%) "*P* and *T* ambient"	Proportion (%) "without molecular water" drying at 105 °C
Montmorillonite	70.6±2.7	79.2±3.0
Phlogopite 1M	2.7±2.7	3.0±3.0
Pyrite	0.5	0.6
Calcite	0.7±0.5	0.8±0.6
Ankérite	1.0±0.3	1.1±0.4
Anatase	0.1	0.1
Plagioclase	8.2±2.7	9.2±3.0
Feldspath K	1.8±1.8	2.0±2.0
Phosphate	0.6	0.6
Quartz+cristobalite	2.5±2.5	2.8±2.8
Fe_2O_3	0.4±0.3	0.5±0.4
Molecular water	10.8	–
Organic carbon	0.1	0.1
Total	100	100

ICP-MS and other complementary analysis (Sauzeat et al., 2001).

ical composition obtained by this method permitted a structural formula estimation:

$$(Si_{3.99}Al_{0.01})(Al_{1.5413}Mg_{0.2448}Fe(III)_{0.1893}) \times Na_{0.2186}Ca_{0.057}O_{10}(OH)_2$$

This structural formula corresponds to a low charge montmorillonite with mixed "Na–Ca" filling interlayer.

ICP-MS and other complementary analyses for chemical composition were used to estimate the mineral composition of the MX80 bentonite (Table 1).

2.2. ESEM methodology

For all environmental scanning electron microscope investigations, an XL30 ESEM LaB6 (FEI and Philips) was used, with a gaseous secondary electron detector (GSED) to produce a surface image. This microscope is also equipped with a "cooling stage" to control the sample temperature.

ESEM manipulation to study the swelling–shrinkage kinetics consists basically of three stages.

2.2.1. Drying

The chamber pressure and sample temperature are fixed at 2.3 Torr and 50 °C, respectively. In this case, the relative humidity of the sample is 2.5% according to the water phases diagram. The sample is maintained at these "reference conditions" for about 15 min, and an image of an aggregate of interest is chosen and stored in the hard disk of the control PC.

2.2.2. Swelling

The chamber pressure and the sample temperature are simultaneously set at 8.2 Torr and 9 °C, respectively, and images are immediately taken approximately every 30 s for 10 min.

2.2.3. Shrinkage

Here, the chamber pressure and sample temperature are again brought back at reference conditions

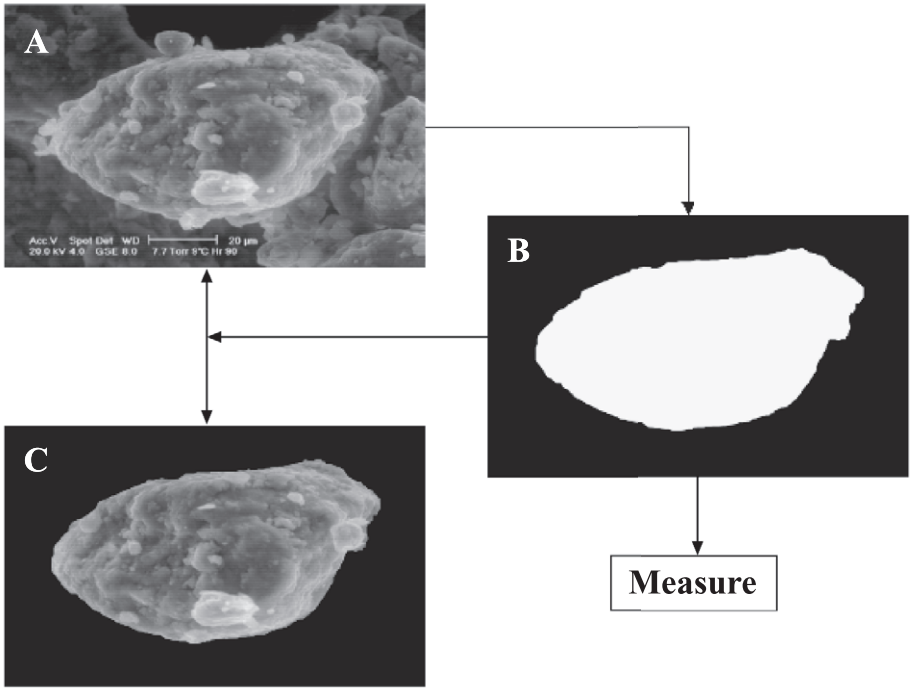

Fig. 1. Digital image analysis methodology. (A) ESEM image; (B) image binarization and isolation of the surface "aggregate" of interest; (C) image reconstitution and control verification.

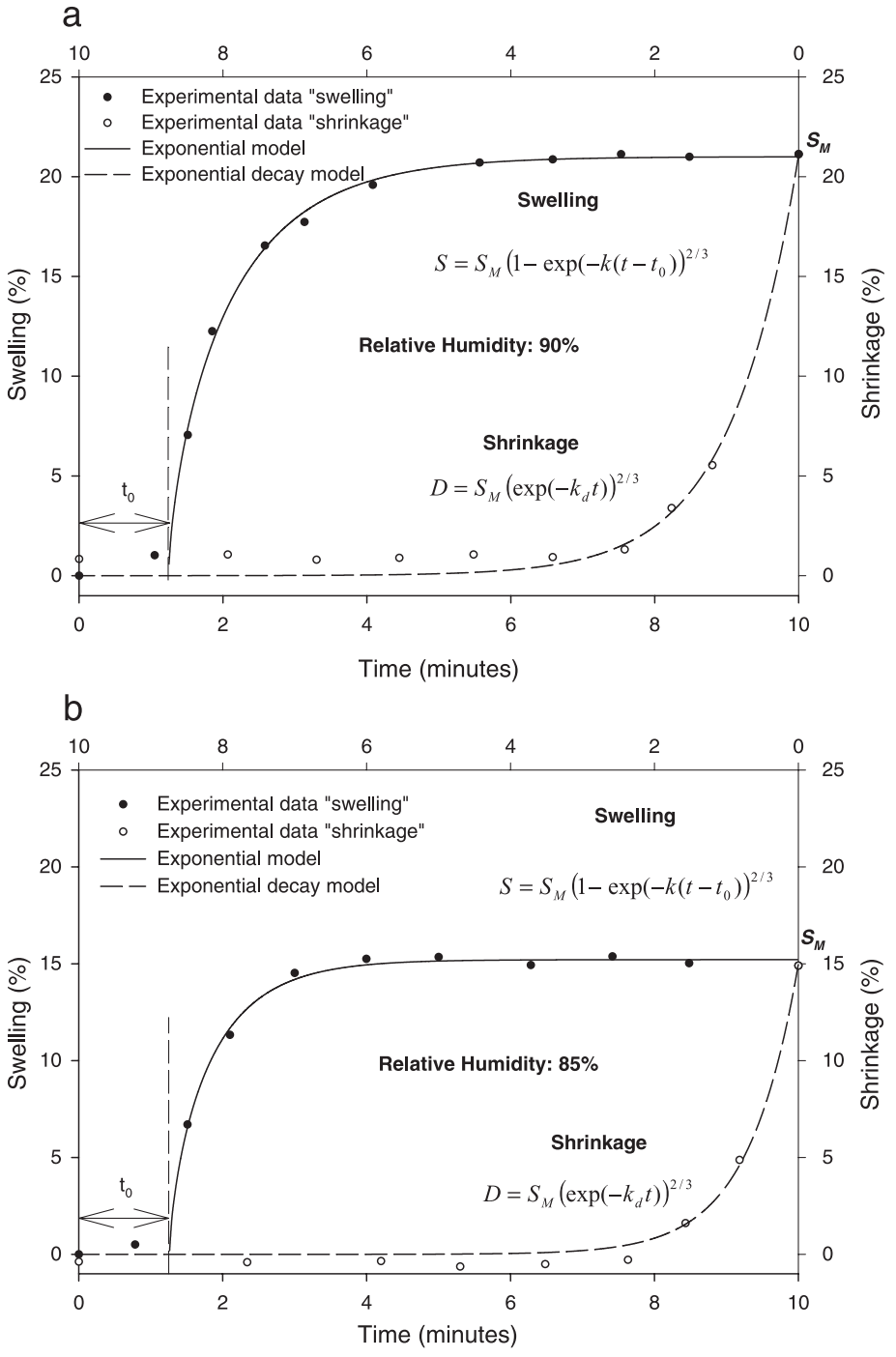

Fig. 2. (a, b, c, d, e, f, g, h) Swelling–shrinkage cycles of the MX80 bentonite at eight relative humidities (55%, 60%, 65%, 70%, 75%, 80%, 85%, 90%). Experimental data fitted by exponential models.

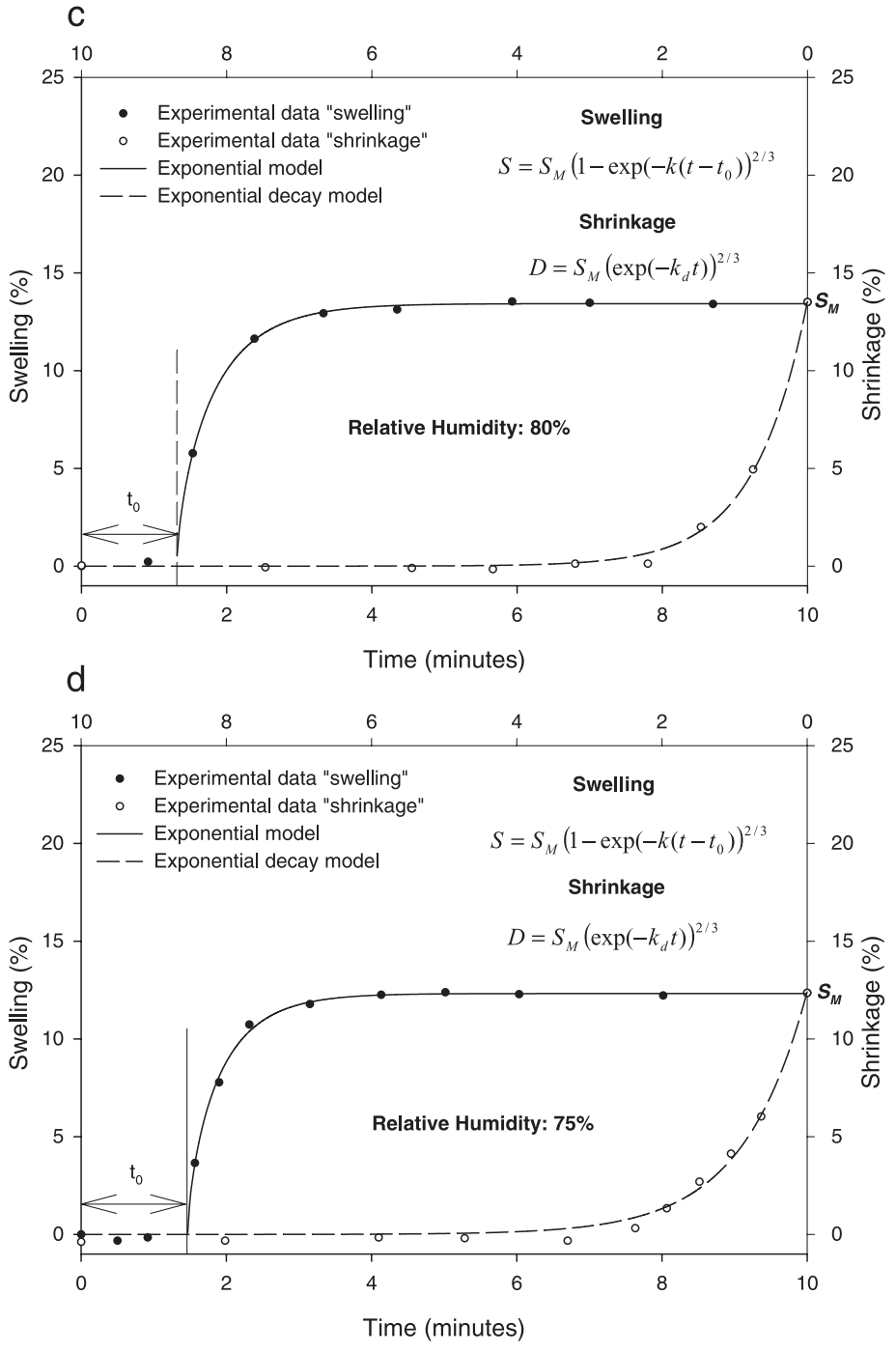

Fig. 2 (*continued*).

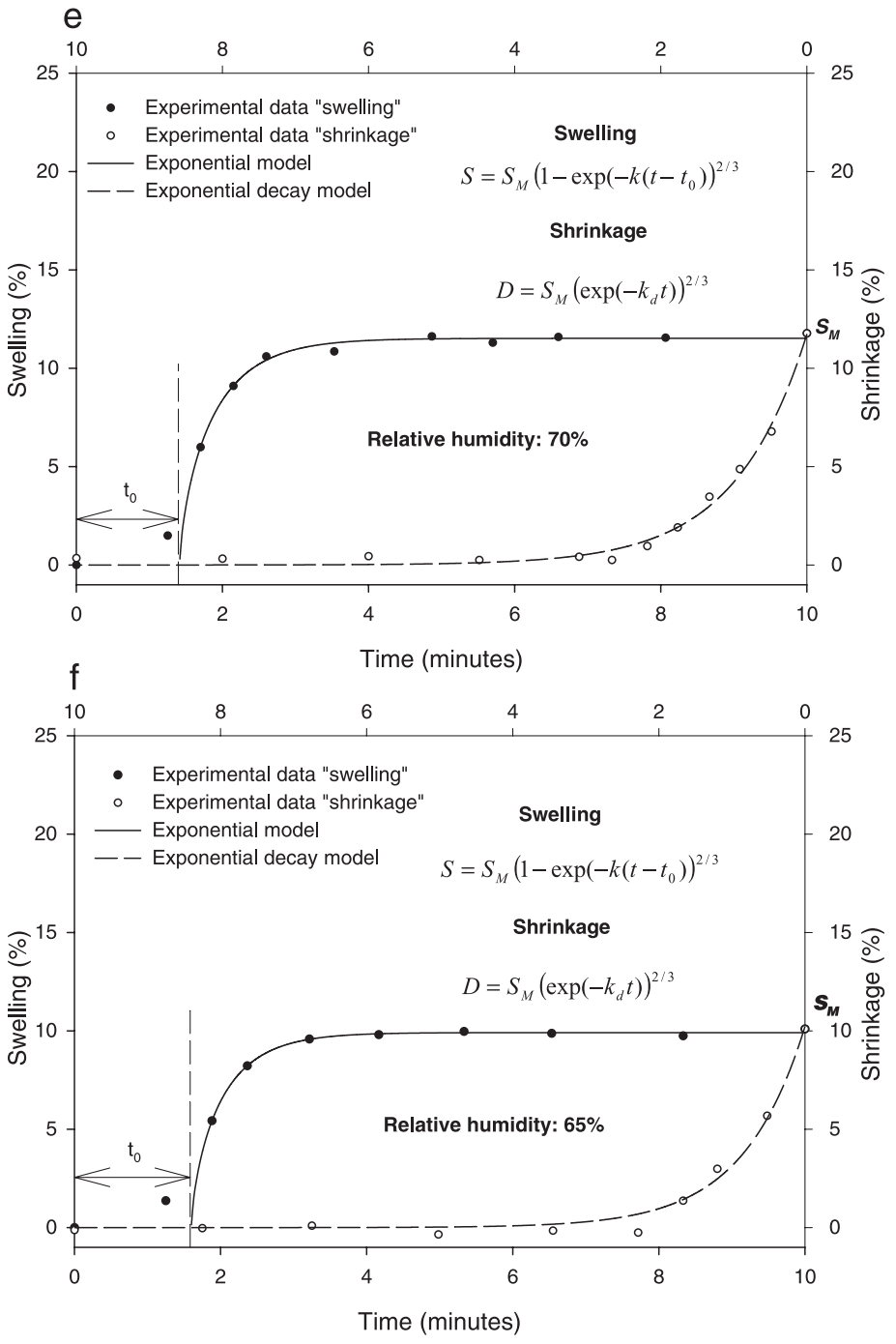

Fig. 2 (*continued*).

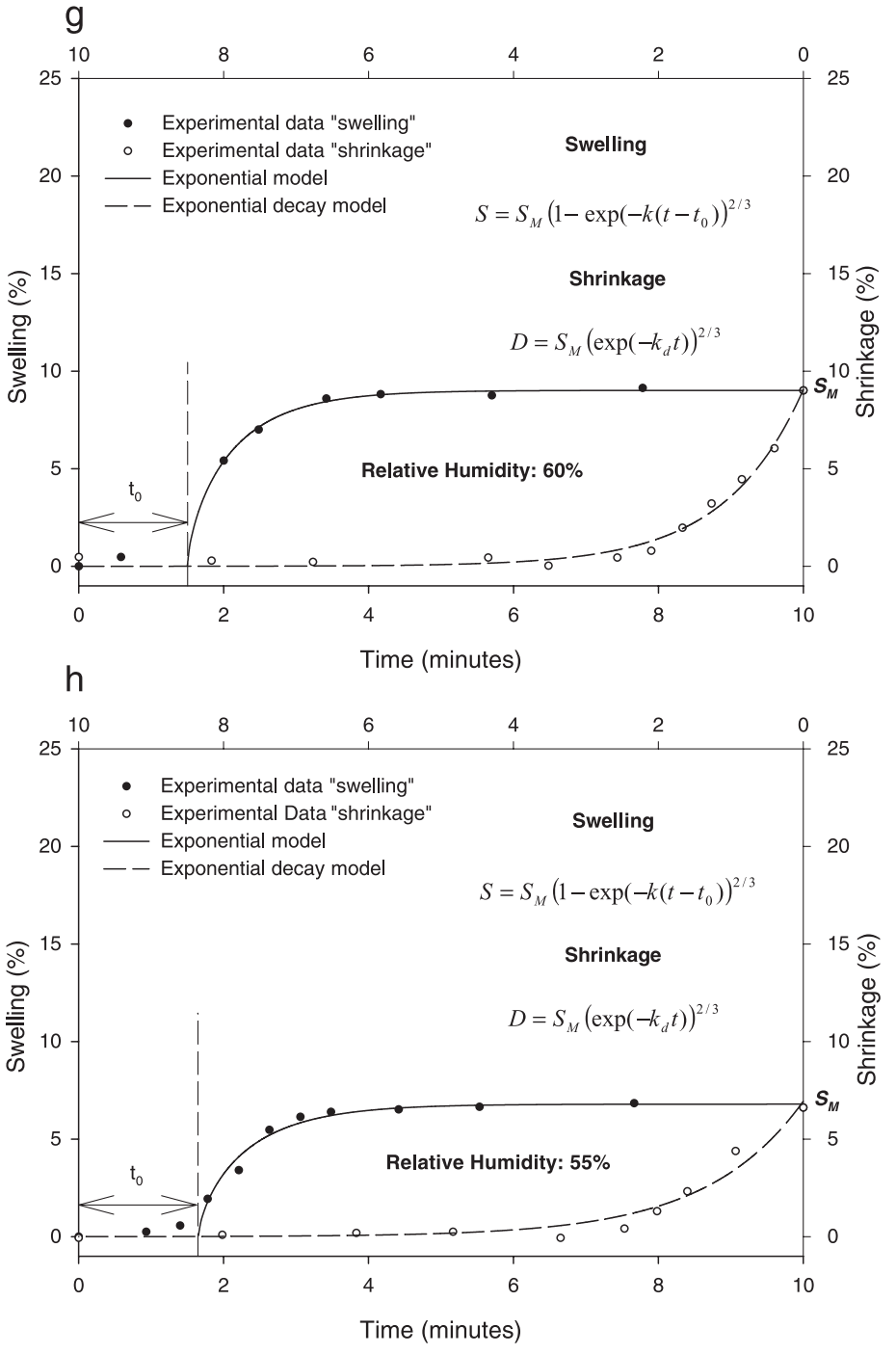

Fig. 2 (*continued*).

(P=2.3 Torr and T=50 °C). The image acquisition is also done as a function of time for 10 min.

This kinetic procedure of swelling–shrinkage was applied on the same aggregate at nine relative humidities (95%, 90%, 85%, 80%, 75%, 70%, 65%, 60%, 55%). It was also applied with four aggregates of the different sizes at 80% of relative humidity.

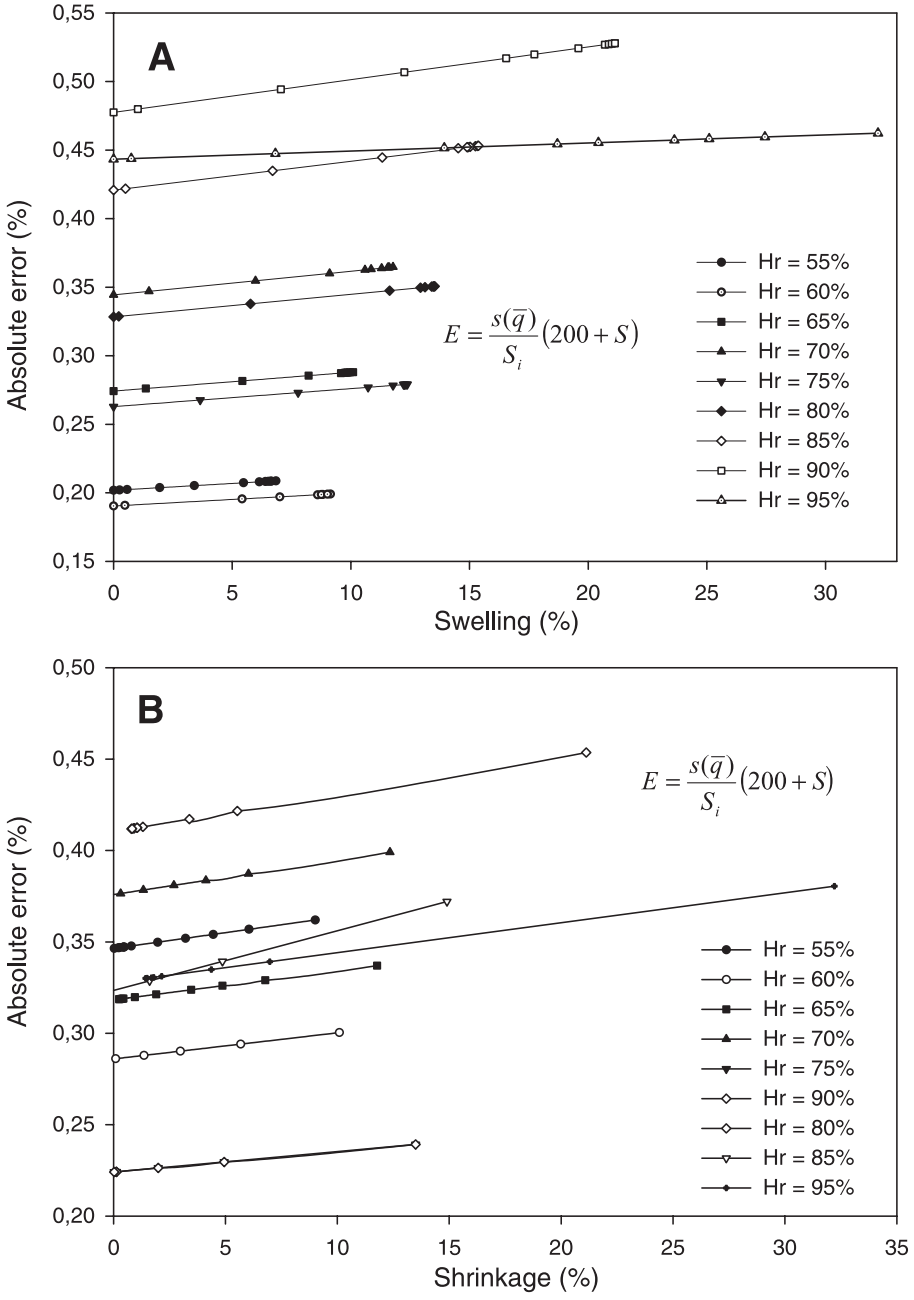

Fig. 3. Absolute error behavior: (A) Swelling; (B) shrinkage.

2.3. DIA methodology

Digital image analysis allows of isolating an area of interest by a commercial software (Visilog 5.3). In this study, aggregates were always the area of interest.

Generally, the ESEM images have sufficient density contrast to apply a simple gray level threshold to isolate the area of interest. To minimize the experimental error on the measure (surface), the same procedure was applied manually five times. In addition each analysis was visually controlled by the reconstitution of binary image (Fig. 1).

The ESEM images of the test section occupied about 1424×968 pixels, and in all measurements, the same gray level range "0–256" has been considered.

3. Results and discussion

3.1. Experimental data

The experimental swelling–shrinkage data are derived from digital image analysis "bi-dimensional analysis". The results are shown as surface augmentation and/or diminution as function of time. The swelling–shrinkage percentage is then estimated by:

$$S = \frac{S_t - S_{\mathrm{i}}}{S_{\mathrm{i}}} 100 \qquad (1)$$

where S_t represents the surface at a t instant time and S_{i} represents the initial reference surface.

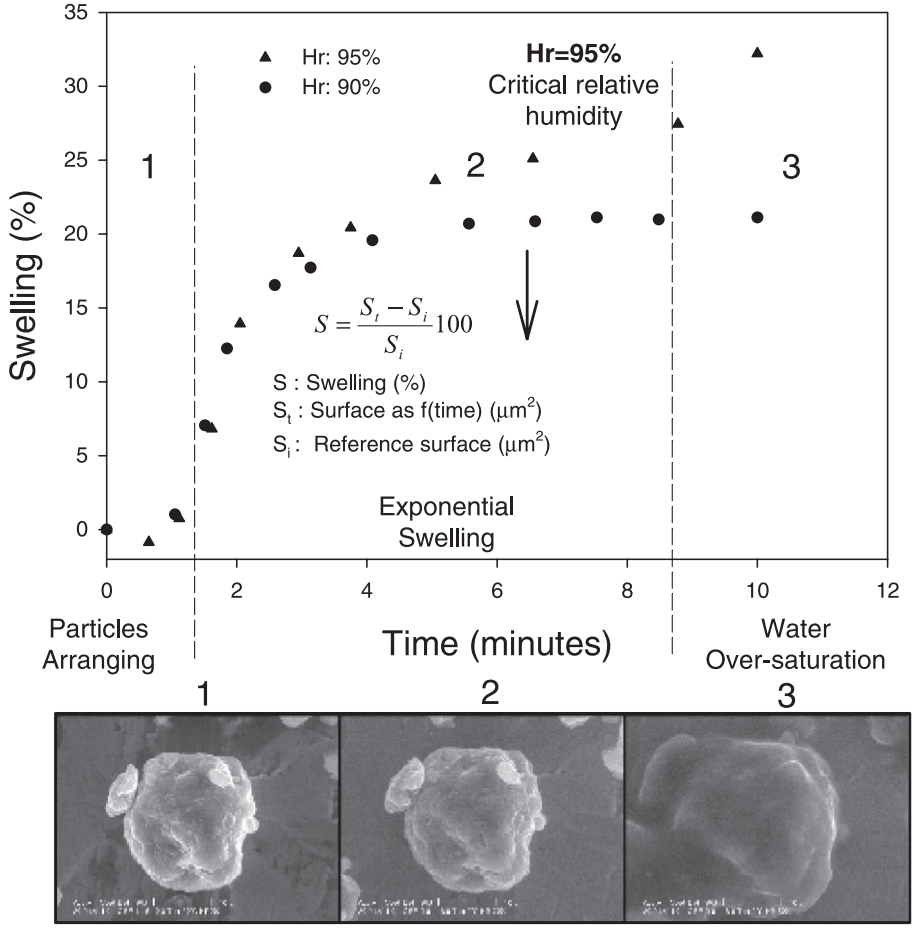

Fig. 4. Swelling kinetic of bentonite "aggregate". Determination by coupled ESEM–DIA (Montes-H, 2002).

Fig. 2 shows the experimental swelling–shrinkage data concerning eight cycles at different relative humidities.

3.2. Measurements precision

The average standard deviation obtained after five repeated surface measurements was considered as an estimate of the absolute error on swelling–shrinkage.

$$E = \frac{s(\bar{q})}{S_i}(200 + S) \quad (2)$$

where $s(\bar{q})$ is the average standard deviation, S_i is the initial surface and S is the swelling–shrinkage percentage.

The absolute error remains relatively low. However, the error is always more significant at low relative humidity (Fig. 3).

3.3. Curve fitting

3.3.1. Swelling

The experimental data were fitted using a kinetic model of the first order:

$$\frac{dw}{dt} = k(w_M - w) \quad (3)$$

This kinetic model represents the volume augmentation as a function of time up to a asymptotic maximum of time. The integral form is represented by an exponential equation:

$$w = w_M(1 - \exp(-kt)) \quad (4)$$

This equation can only be applied when volume varies. Unfortunately, the measurement estimated in this study corresponds to surface variations, and not to volume variations. If we consider that the swelling–shrinkage of the bentonite is equi-dimensional at an aggregate scale, the Eq. (4) can be written in terms of surface:

$$S = S_M(1 - \exp(-kt))^{2/3} \quad (5)$$

The experimental data shows that the swelling kinetic of "aggregates of the bentonite (MX80)" can be defined by three stages (Fig. 4). The first stage is very difficult to model, because of the random arrangement of the particles in the initial water adsorption. In general this stage is characterized by a non-swelling feature and sometimes by an aggregate contraction. The second stage presents a high swelling during first minute, after the swelling decreases gradually up to a asymptotic maximum of time. This stage may be modeled by an exponential Eq. (5). The third stage is only presented at a critical relative humidity. Here it is produced as the "water over-saturation of an aggregate" with a critical relative humidity of 95%.

The final equation to fit only the second stage of bentonite swelling is then:

$$S = S_M(1 - \exp(-k(t - t_0))^{2/3} \quad (6)$$

where S_M is the maximum swelling (%), k is the coefficient of the swelling (1/min), and t_0 is the initial time of the exponential swelling.

3.3.2. Shrinkage

The shrinkage behaviour comprises one stage, which may be modeled by a exponential decay model. The final equation in terms of surface is:

$$D = S_M(\exp(-k_d t))^{2/3} \quad (7)$$

where S_M is the maximum swelling (%) and k_d is the coefficient of the shrinkage (1/min).

Fig. 2 shows experimental data and fitting curves for eight swelling–shrinkage cycles at different relative humidities. In addition, the fitting parameters are showed in Tables 2 and 3. These parameters were estimated by non-linear regression using least-squares method.

Table 2
Fitting kinetic parameters

Humidity (%)	Fitting parameters			Regression coefficient, R
	S_M (%)	k (1/min)	t_0 (min)	
90	20.99	0.88	1.24	0.9978
85	15.21	1.33	1.26	0.9955
80	13.43	1.50	1.31	0.9992
75	12.32	1.75	1.46	0.9983
70	11.51	1.66	1.41	0.9936
65	9.91	1.84	1.60	0.9980
60	9.01	1.23	1.50	0.9953
55	6.79	1.13	1.65	0.9841

Bentonite swelling at eight relative humidities. Nonlinear regression by least-squares method (Montes-H, 2002).

Table 3
Fitting kinetic parameters

Humidity (%)	Fitting parameters		Regression coefficient, R
	S_M (%)	k (1/min)	
90→2.5	21.04	1.61	0.9940
85→2.5	14.95	2.16	0.9954
80→2.5	13.53	2.05	0.9988
75→2.5	12.40	1.68	0.9959
70→2.5	11.71	1.53	0.9956
65→2.5	10.20	1.77	0.9932
60→2.5	9.05	1.40	0.9930
55→2.5	6.93	1.12	0.9784

Bentonite shrinkage at eight relative humidities. Nonlinear regression by least squares method (Montes-H, 2002).

3.4. Discussion

3.4.1. Method validation

With direct observations with ESEM and with digital image analysis, it was possible to identify three swelling stages (Fig. 4). The first and second stages were also identified by the mechanical methods for other expansive clays (Al-Rawas, 1998; Wild et al., 1999).

The exponential models used to fit the swelling–shrinkage, are very well correlated with the experimental data since the coefficients of nonlinear regression estimated are close to 1 (Tables 2 and 3). This may be an indirect reason to confirm that the swelling–shrinkage is effectively equi-dimensional. The second reason to confirm the equi-dimensionality of the swelling–shrinkage "aggregate scale" is done by digital image analysis which shows a linear correlation between the width and the length of the aggregate (Fig. 5).

3.4.2. Swelling curves

The maximum swelling values S_M estimated by the theoretical model for each relative humidity are very close to the experimental values. It was evident that the maximum swelling depends directly on the relative humidity (Fig. 6).

The swelling rate is determined by the k swelling coefficient. This parameter depends on several factors. For example, Fig. 7 shows that the swelling coefficient decreases linearly when the relative humidity increases. It signifies that at high relative humidity, it takes more time to reach maximum swelling. The

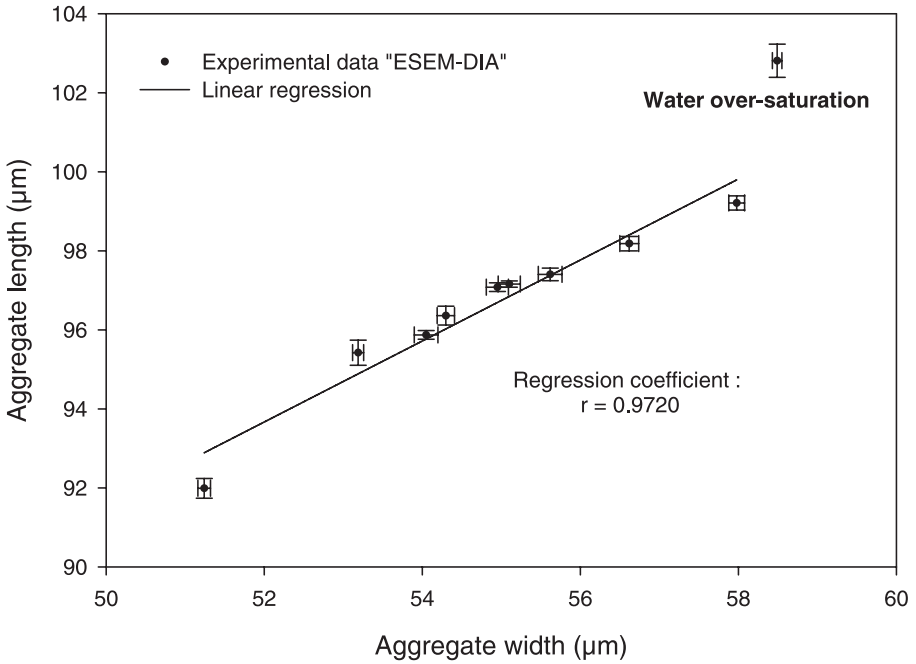

Fig. 5. Aggregate width and length correlation on the swelling–shrinkage. Estimation by digital image analysis (DIA).

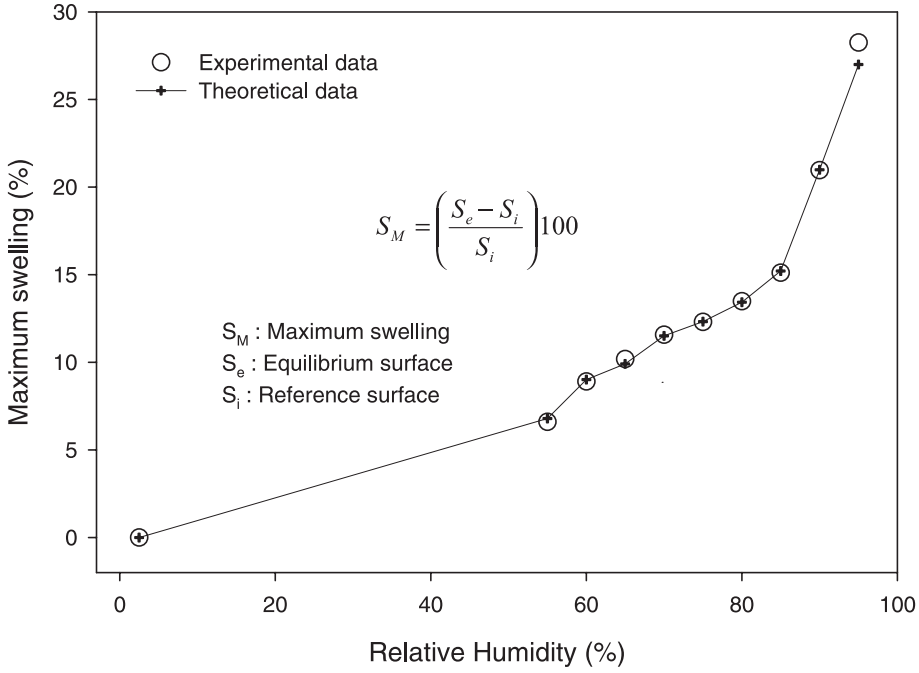

Fig. 6. Swelling isotherm. Experimental data and theoretical data comparison "exponential model".

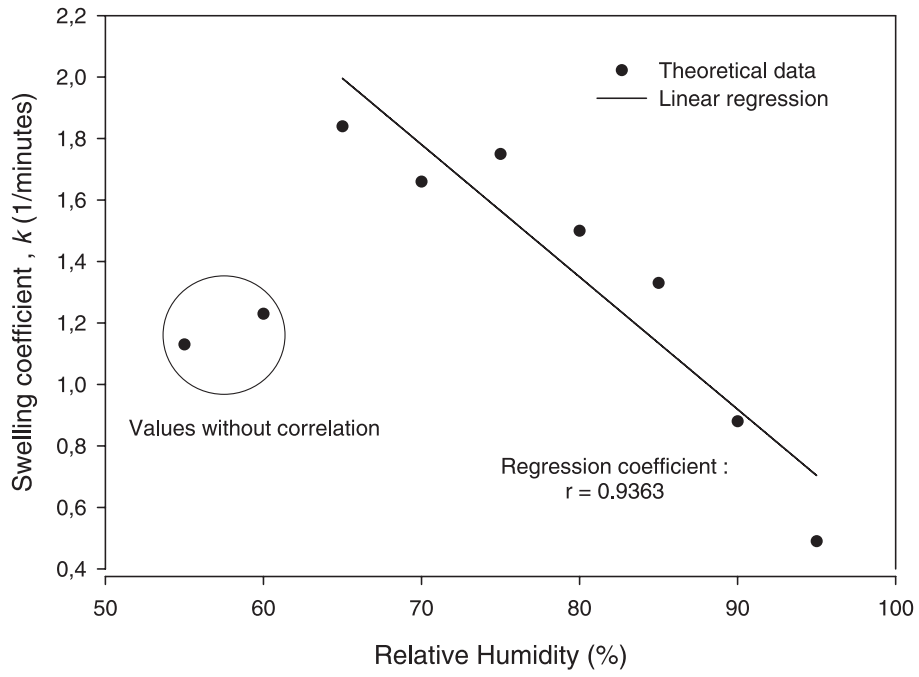

Fig. 7. The *k* swelling coefficient and relative humidity correlation. The *k* values are obtained by nonlinear regression "least-squares method" on the exponential model.

negative linear correlation is only valid between 65% and 95% relative humidity. At lower relative humidity, the two swelling coefficient values do not present a correlation. This may be due to a decreasing swelling at low relative humidities. The coefficient of swelling also depends on the aggregate size. Fig. 8 shows that the coefficient of swelling decreases approximately linearly as the aggregate size increases. This linear correlation is only valid between 1800 and 7500 μm^2. The aggregates of low size do not present an uniform kinetic behaviour. Several experiences show a nearly instantaneous water over-saturation (for aggregates <100 μm^2), where the maximum swelling is low and there is very high sensitivity to the aggregate deformation. This may be due to the texture of the small aggregates, which are generally more compact. The inter-particle porosity is then lower, and during hydration, the slightly modified inter-particle porosity induces a lower aggregate swelling.

It is evident that the coefficient of swelling also depends on the nature of interlamellar cations and on the nature and composition of the expansive clay. These parameters are not evaluated in this study.

Finally, the parameter t_0 was defined to estimate the time at which the exponential swelling begins. Fig. 9 shows that t_0 decreases slightly when the relative humidity increases. That may be logical because the diffusion coefficient of water vapour is directly proportional to the relative humidity.

3.4.3. Shrinkage curves

The shrinkage model shown here contains only two fitting parameters, S_M and k_d. The maximum swelling S_M is the same fitting parameter used for shrinkage and swelling models. The S_M estimations show a very good correlation between the two models (see Tables 2 and 3). On the other hand, the coefficient of shrinkage seems not to depend on the relative humidity. In fact, the shrinkage rate is similar under almost all relative humidities.

3.4.4. Comparison between swelling and shrinkage curves

In general, the swelling rate is higher than the shrinkage rate only when the "second stage" exponential swelling is considered. However, when the time taken by the first stage t_0 is also considered, it is

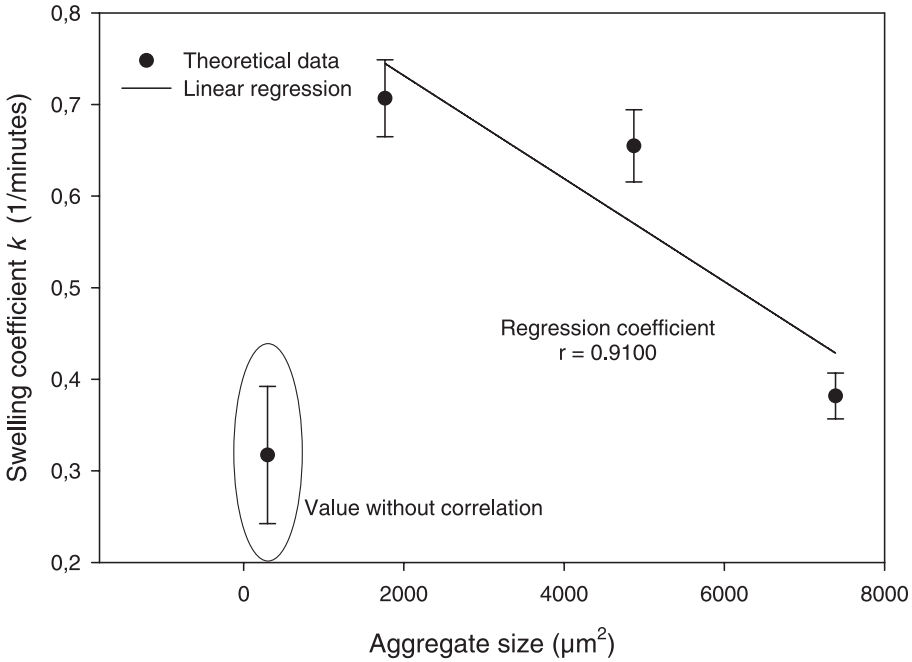

Fig. 8. The k swelling coefficient and aggregate size correlation. Aggregate size estimation by DIA.

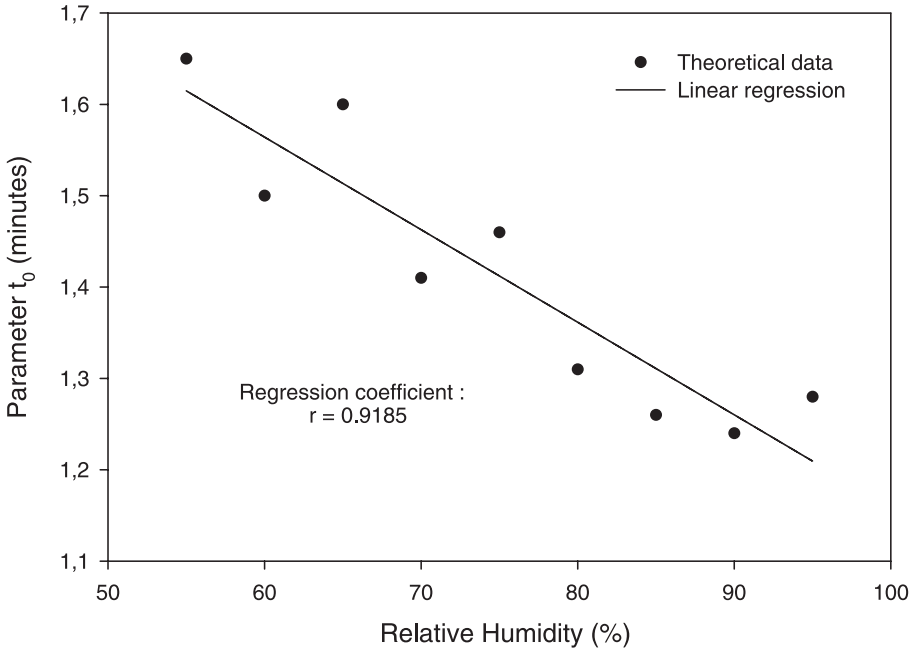

Fig. 9. Correlation between the initial time before exponential swelling, t_0, and relative humidity. (The t_0 values are obtained by nonlinear regression "least squares method" on the exponential model).

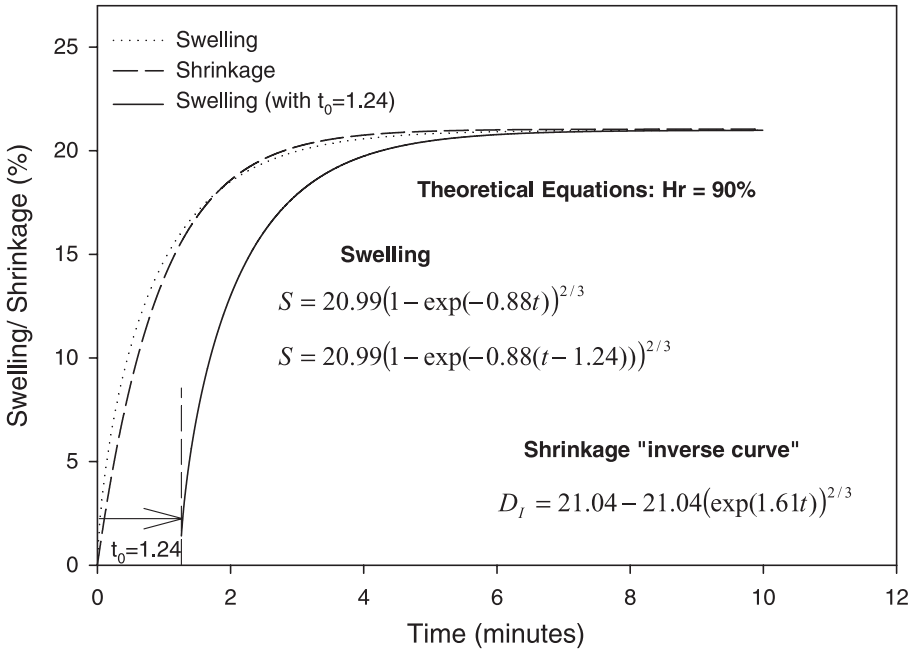

Fig. 10. Comparison between the theoretical swelling and shrinkage curves at 90% relative humidity. The theoretical shrinkage curve was reversed.

noticed that the swelling rate is much lower than the shrinkage rate. Fig. 10 shows a comparative example between the swelling and shrinkage curves at 90% relative humidity. It was necessary to reverse the shrinkage curve for this comparison.

4. Conclusions

Three main conclusions can be given in this work.

First, the results show that the coupling environmental scanning electron microscopy (ESEM) with digital images analysis (DIA) is a powerful method to estimate the swelling–shrinkage potential of expansive clays. The main advantage of this method is the rapidity with which one obtains the qualitative and quantitative results. However, this method allows only to estimate the free swelling/shrinkage potential in the sample chamber.

Second, thanks to the direct observations with ESEM it was possible to identify three steps for the swelling kinetic: (1) particles arrangement; (2) exponential swelling; (3) water over-saturation. In addition, the exponential models and the digital "2D" image analysis confirm that the swelling–shrinkage potential of the MX80 bentonite is equi-dimensional "aggregate scale".

Third, it was possible to demonstrate that the shrinkage speed is widely higher that the swelling speed thanks to the exponential models.

Acknowledgements

The authors are grateful to the National Council of Science and Technology, Mexico, and the Louis Pasteur University, France, for providing a financial grant for this work.

References

Abdullah, W.S., Abdullah, W.S., Alshibli, K.A., Al-Zou'bi, M.S., 1999. Influence of pore water chemistry on the swelling behavior of compacted clays. Appl. Clay Sci. 15, 447–462.

Al-Rawas, A.A., 1998. The factors controlling the expansive nature of the soils and rocks of northern Oman. Eng. Geol. 53, 327–350.

Al-Tabbaa, A., Aravinthan, T., 1998. Natural clay-shredded tire mixture as landfill barrier materials. Waste Manage. 18, 9–16.

Baker, J.C., Grabowska-Olszewska, B., Uwins, J.R., 1995. ESEM study of osmotic swelling of bentonite from Radzionkow (Poland). Appl. Clay Sci. 9, 465–469.

Jenkins, L.M., Donald, A.M., 2000. Observing fibers swelling in water with an environmental scanning electron microscope. Textile Res. J. 70, 269–276.

Komine, H., Ogata, N., 1994. Experimental study on swelling characteristics of compacted bentonite. Can. Geotech. J. 31, 478–490.

Montes-H, G., 2002. Etude expérimentale de la sorption d'eau et du gonflement des argiles par microscopie électronique à balayage environnementale (ESEM) et analyse digitale d'images. PhD thesis, Louis Pasteur University, Strasbourg I, France.

Murray, H.H., 2000. Traditional and new applications for kaolin, smectite, and palygorskite: a general overview. Appl. Clay Sci. 17, 207–221.

Parcevaux, P., 1980. Etude microscopique et macroscopique du gonflement de sols argileux. PhD thesis, Pierre et Marie Curie University, Paris VI. 266 pp.

Pusch, R., 1992. Use of bentonite for isolation of radioactive waste products. Clay Miner. 27, 353–361.

Sauzeat, E., Guillaume, D., Neaman, A., Dubessy, J., François, M., Pfeiffert, C., Pelletier, M., Ruch, R., Barres, O., Yvon, J., Villéras, F., Cathelineau, M., 2001. Caractérisation minéralogique, cristallochimique et texturale de l'argile MX80. Rapport ANDRA No. CRP0ENG 01-001. 82 pp.

Wild, S., Kinuthia, J.M., Jones, G.I., Higgins, D.D., 1999. Suppression of swelling associated with ettringite formation in lime stabilized sulphate bearing clay soils by partial substitution of lime with ground granulated blast-furnace slag. Eng. Geol. 51, 257–277.